



Cite this: *Chem. Commun.*, 2017, 53, 12357

Received 24th September 2017,
Accepted 27th October 2017

DOI: 10.1039/c7cc07452b

rsc.li/chemcomm

Near-UV excitation of non-heme $\text{Fe}^{\text{IV}}=\text{O}$ complexes results in light intensity dependent increase in reaction rates for the oxidation of C–H bonds even at low temperature ($-30\text{ }^{\circ}\text{C}$). The enhancement of activity is ascribed to the ligand-to-[$\text{Fe}^{\text{IV}}=\text{O}$] charge transfer character of the near-UV bands to generate a highly reactive $[(\text{L}^{\text{+}})\text{Fe}^{\text{III}}-\text{O}^{\text{*}}]$ species. The enhancement is not observed with visible/NIR excitation of the d–d absorption bands.

The photochemistry of iron complexes saw a spurt of interest in the 1960s,^{1–3} but this interest was rapidly superseded by the photochemistry of Ru(II) complexes, of which the paradigm is $[\text{Ru}(\text{bpy})_3]^{2+}$, due to the latter's long lived excited states and luminescence.¹ Indeed the photochemistry of these complexes has seen recent further interest in photo-redox catalysis, driven largely by the access they provide to novel SOMO reactivity and, to a lesser extent, in inorganic oxidation catalysis by the possibility of generating reactive intermediates directly without the use of terminal oxidants such as *m*CPBA, PhIO, H_2O_2 etc. $[\text{Ru}(\text{bpy})_3]^{2+}$ has been employed as a photo-oxidant to generate high-valent metal-oxido species that can engage in selective oxidation of C–H and C=C bonds. In 2011, Fukuzumi, Nam and co-workers reported the first example of photocatalytic formation of $[(\text{N}4\text{Py})\text{Fe}^{\text{IV}}=\text{O}]^{2+}$ (**1**)⁴ from step-wise electron transfer oxidation of $[(\text{N}4\text{Py})\text{Fe}^{\text{II}}(\text{CH}_3\text{CN})]^{2+}$ (**1a**) by visible light generated photo-excited Ru(II) complexes.^{5,6} The C–H oxidation carried out *in situ* by hydrogen atom abstraction (HAT) with **1** is the rate determining step, which places an upper limit on the overall efficiency of the system.^{7,8} It is notable, however, that complexes such as $[(\text{N}4\text{Py})\text{Fe}^{\text{II}}(\text{CH}_3\text{CN})]^{2+}$ (**1a**) undergo oxidation to their corresponding Fe(III) complexes (**1b**) upon irradiation in water or in methanol.⁹ Hence, the photo-redox behaviour of iron

Direct photochemical activation of non-heme $\text{Fe}^{\text{IV}}=\text{O}$ complexes†

Juan Chen,^a Apparao Draksharapu,^{id ab} Emma Harvey,^a Waqas Rasheed,^{id b} Lawrence Que Jr.^{id *b} and Wesley R. Browne^{id *a}

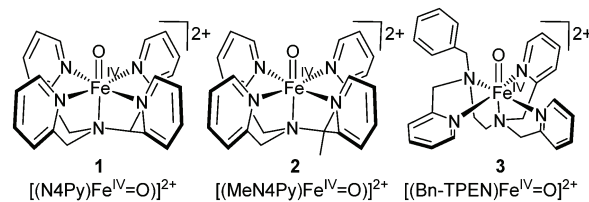


Fig. 1 Structures of $\text{Fe}^{\text{IV}}=\text{O}$ complexes discussed in the text.

complexes in general deserves attention also in the context of light driven oxidation chemistry.

Here we report the wavelength-dependent direct photochemical activation of a series of non-heme iron(IV)-oxo complexes $[(\text{N}4\text{Py})\text{Fe}^{\text{IV}}=\text{O}]^{2+}$ (**1**),⁴ $[(\text{MeN}4\text{Py})\text{Fe}^{\text{IV}}=\text{O}]^{2+}$ (**2**), and $[(\text{Bn-TPEN})\text{Fe}^{\text{IV}}=\text{O}]^{2+}$ (**3**) (Fig. 1)† in the absence and presence of oxidisable substrates, both in acetonitrile and in methanol. Although excitation into the NIR absorption bands of complexes **1–3** has no discernible effect on the reactivity of these complexes, excitation into near-UV charge transfer bands results in a light-intensity-dependent enhancement of the oxidative reactivity of these complexes towards C–H bonds.

The self-decay of **1** to **1a** in the dark in acetonitrile is negligible over 1 h at $21\text{ }^{\circ}\text{C}$ ($5.8 \times 10^{-5}\text{ s}^{-1}$, Fig. S1, ESI†), in accordance with earlier reports.⁷ Irradiation of **1** in acetonitrile at 365 nm (Fig. 2), however, results in a decrease in absorbance at 696 nm, the rate of which is dependent on light intensity (with an overall quantum yield of >0.006 , Fig. S1, ESI†). The loss in absorbance at 696 nm is followed, after a delay, by an increase in absorbance at 378 and 454 nm, corresponding to formation of the Fe(II) complex $[(\text{N}4\text{Py})\text{Fe}^{\text{II}}(\text{CH}_3\text{CN})]^{2+}$ (**1a**). Comparison with an independently prepared solution of **1a** (Fig. S2, ESI†) confirms $>95\%$ overall conversion to **1a** and that reduction of **1** does not result in ligand degradation. The rate of photoreduction of **1** in acetonitrile is not obviously affected by the presence or absence of dioxygen (Fig. S3, ESI†), nor is it affected by solvent deuteration (CD_3CN , Fig. S4, ESI†).

The total concentration (**1** + **1a**, Fig. 2, blue trace) calculated from the absorbance at 696 nm and 454 nm (where the spectra

^a Stratingh Institute for Chemistry, Faculty of Science and Engineering, Nijenborgh 4, 9747AG, Groningen, The Netherlands. E-mail: w.r.browne@rug.nl

^b Department of Chemistry and Center for Metals in Biocatalysis, University of Minnesota, 207 Pleasant St. SE, University of Minnesota, Minneapolis, MN55455, Minnesota, USA. E-mail: larryque@umn.edu

† Electronic supplementary information (ESI) available: Experimental details, additional spectroscopy data. See DOI: 10.1039/c7cc07452b

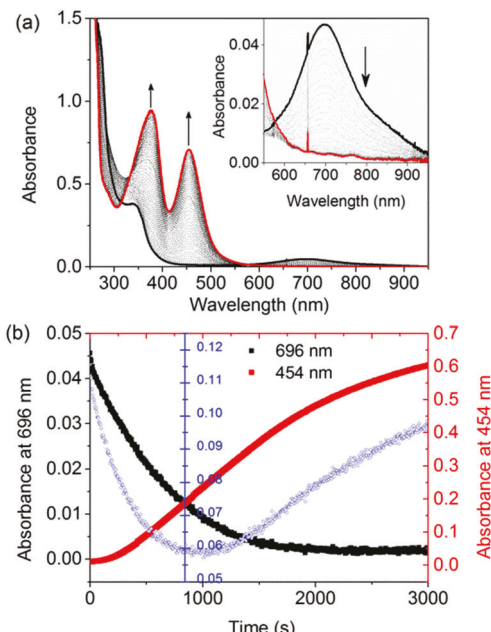
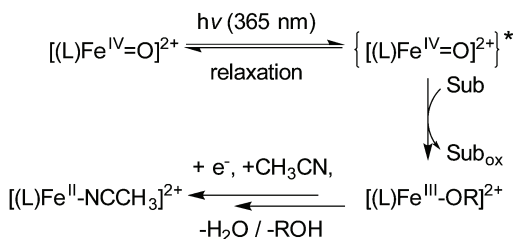


Fig. 2 (a) UV-vis absorption spectrum of **1** (0.125 mM) in acetonitrile at 21 °C before (black) and during irradiation at 365 nm (dashed lines) with the final spectrum in red. Inset: Expansion from 550 to 950 nm. (b) Absorbance at 696 nm (black, left y-axis) and 454 nm (red, right y-axis) over time. The total concentration of **1** ($\text{Fe}^{\text{IV}}=\text{O}$) and **1a** ($\text{Fe}^{\text{II}}(\text{CH}_3\text{CN})$) (blue, centred y-axis) was calculated from the absorbance at 696 nm ($\epsilon_{696\text{ nm}} \mathbf{1} = 400 \text{ M}^{-1} \text{ cm}^{-1}$) and at 454 nm ($\epsilon_{454\text{ nm}} \mathbf{1a} = 6520 \text{ M}^{-1} \text{ cm}^{-1}$).¹⁰

of **1** and **1a** show negligible overlap) shows an initial rapid decrease (within 900 s) followed by a slower increase. These data indicate that the photoreduction from the $\text{Fe}(\text{IV})$ to the $\text{Fe}(\text{II})$ redox state is a multi-step process (Scheme 1). The intermediate species formed (*i.e.* the $\text{Fe}(\text{III})$ complex, **1b**) do not show significant visible absorption, which is consistent with the lack of an isosbestic point throughout the irradiation. Furthermore the initial increase and subsequent decrease in absorbance at 310 nm (Fig. 2a) is consistent with the intermediacy of **1b**.

EPR spectra (Fig. S5, ESI†) show that the initial decrease of **1** results in the formation of primarily one low-spin Fe^{III} species, $[(\text{N4Py})\text{Fe}^{\text{III}}-\text{X}]^{2+}$ ($g = 2.29, 2.12, 1.96$), as well as minor amounts of low-spin $[(\text{N4Py})\text{Fe}^{\text{III}}-\text{OH}]^{2+}$ ($g = 2.41, 2.16, 1.92$) and high-spin $[(\text{N4Py})\text{Fe}^{\text{III}}-\text{OH}_2]^{2+}$. Double integration and comparison



where $\text{L} = \text{N4Py}$, MeN4Py and Bn-TPEN

Scheme 1 Initial reaction of photo-excited $\text{Fe}(\text{IV})=\text{O}$ complexes results in thermal relaxation or reduction to their $\text{Fe}(\text{III})-\text{OR}$ analogues (**1b**, $\text{R} = \text{H}$, alkyl), which undergoes subsequent slower reduction together with ligand exchange to form, *e.g.*, **1a**.

with the spectrum of the low-spin Fe^{III} species **1b** shows that the decrease in concentration of **1** in acetonitrile is approximately equal to the increase in concentration of a low-spin Fe^{III} species and the Fe^{II} complex **1a**.

The structurally related $\text{Fe}^{\text{IV}}=\text{O}$ complex **2** ($[(\text{MeN4Py})\text{Fe}^{\text{IV}}=\text{O}]^{2+}$) shows a similar effect of irradiation as seen for **1** (Fig. 4 and S6, S7).[§] In contrast to **1** and **2**, for $[(\text{BnTPEN})\text{Fe}^{\text{IV}}=\text{O}]^{2+}$ (**3**) a nearly linear decrease in absorbance at 740 nm and concomitant increase in absorbance of an Fe^{II} species at 388 nm are observed, indicating that the second step (Fe^{III} to Fe^{II}) is rapid (Fig. 3).⁷ As for **1**, the rate of reduction of **3** is dependent on the irradiation intensity (Fig. S8, ESI†).

The photoinduced reduction shows a pronounced wavelength dependence. For example, even prolonged intense irradiation (at 490, 565, 660 and 785 nm) into the d-d absorption bands of **2** shows no effect (Fig. 4), in contrast to the photoinduced reduction observed upon irradiation into the LMCT bands (365 and 300 nm, Fig. S6 and S7, ESI†, respectively).

The oxidation of C–H bonds by complexes such as **1–3** has been studied in detail and the thermal reaction is generally accepted to proceed *via* a HAT mechanism, with HAT as the rate determining step.^{7,11} At 21 °C, **1** oxidises substrates such as benzyl alcohol (**BA**), and ethylbenzene (**EB**), with the latter oxidised at a *ca.* 10 times lower rate than the former (Fig. S9 and Table S1, ESI†). In the presence of either substrate (*i.e.* 5 equiv. **BA** or 50 equiv. of **EB**), irradiation in acetonitrile at 21 °C results in a four-fold increase in the rate of loss of NIR absorbance of **1** compared to the thermal reaction and two fold increase (with **BA**)

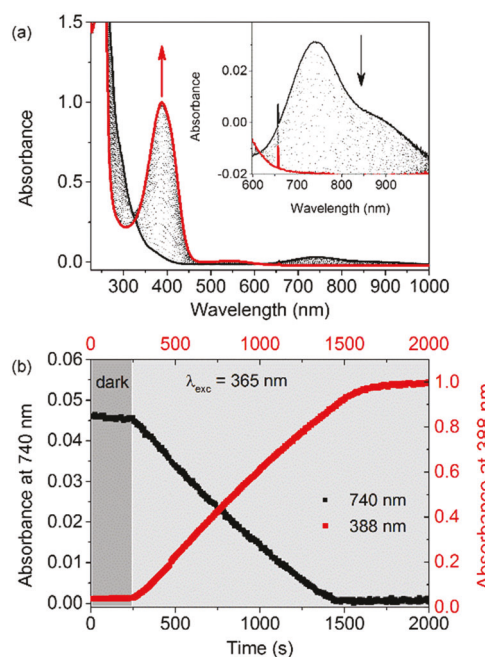


Fig. 3 (a) UV-vis absorption spectrum of **3** (0.125 mM) in acetonitrile at 21 °C before (black) and during irradiation at 365 nm (dashed lines) with the final spectrum in red. Inset: Expansion from 600 to 1000 nm. (b) Absorbance at 740 nm (black, left y-axis) and 388 nm (red, right y-axis) upon irradiation being initiated at 250 s. The slope without irradiation (dark grey stage) is $3.0 \times 10^{-6} \text{ s}^{-1}$ and $4.5 \times 10^{-5} \text{ s}^{-1}$ with irradiation (light grey stage).

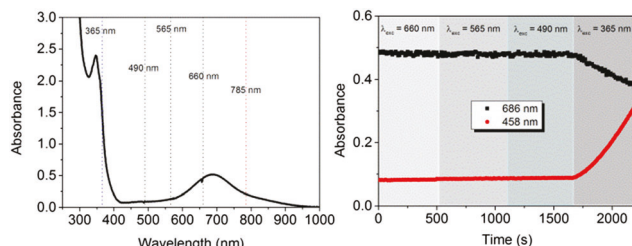


Fig. 4 (a) UV-vis absorption spectrum of **2** (1 mM) in acetonitrile at 21 °C. (b) The corresponding change in absorbance at 686 nm (black) and 458 nm (red) under irradiation at various wavelengths. Irradiation by 785 nm (100 mW) has no effect on the spectrum compared to a non-irradiated samples over 3 h. Slope with irradiation at 660, 565 and 490 nm is $2.7 \times 10^{-6} \text{ s}^{-1}$ and with irradiation at 365 nm is $1.6 \times 10^{-4} \text{ s}^{-1}$.

compared to irradiation of **1** in acetonitrile alone (Table S1, ESI[†]). Notably, the near 10 fold increase in the rate of increase in visible absorbance of **1a** under photo-irradiation in the presence of **BA** indicates that the observed reaction rate is dominated by photokinetics (Table S1, ESI[†]). The oxidation of benzyl alcohol and ethylbenzene under irradiation was confirmed by GC-MS analysis of the reaction mixtures.

At -30°C , the rate of the thermal reaction of **1** with **BA** is reduced substantially¹¹ even with 50 equiv. w.r.t. **1** (2nd order rate constant is $ca. 2.3 \times 10^{-6} \text{ M}^{-1} \text{ s}^{-1}$, Fig. 5 and Fig. S10, ESI[†]). In contrast, the rate of reduction of **1** under irradiation is not affected significantly by the decrease in temperature (Table S2, ESI[†]). Furthermore, although the thermal reaction shows the expected dependence on the concentration of **BA**, the k_{obs} under irradiation is much less sensitive to substrate concentration (Table S2, ESI[†]). Cyclohexanol, which has stronger C-H bonds than benzyl alcohol, shows a similar influence on the rate of decay of **1** under irradiation (Fig. S11 and Table S3, ESI[†]).

Overall the data indicate that, in contrast to the thermal reaction, the overall photochemical reaction rate is dominated by irradiation intensity (*i.e.* photokinetics). The reaction between **1**^{*} (*i.e.* **1** in its electronically excited state) and the substrate competes with non-radiative relaxation to **1**, which is the dominant relaxation pathway. Furthermore, the rate of oxidation of

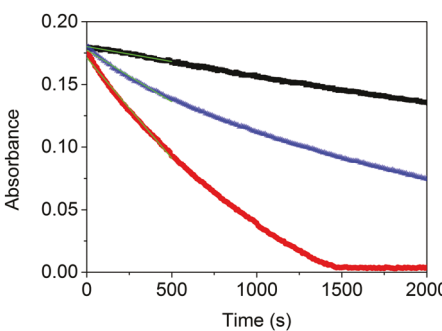
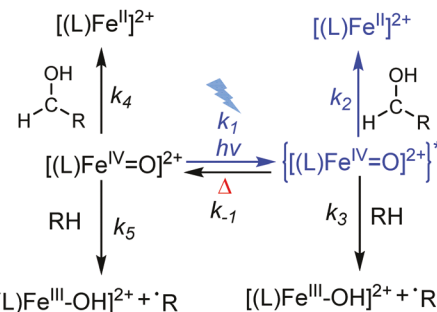


Fig. 5 Absorbance at 696 nm over time of **1** (0.5 mM) in acetonitrile at -30°C : (black) with 50 equiv. benzyl alcohol, (blue) under irradiation (365 nm) without benzyl alcohol, and (red) under irradiation (365 nm) with benzyl alcohol. Linear fitting of the first 500 s shown as yellow lines, slope for thermal reaction is $2.4 \times 10^{-5} \text{ s}^{-1}$, and for photoreaction with benzyl alcohol is $1.6 \times 10^{-4} \text{ s}^{-1}$, without benzyl alcohol is $0.8 \times 10^{-4} \text{ s}^{-1}$.



Scheme 2 Proposed mechanism for photo-activation of **1** towards the substrates oxidation.

BA and cyclohexanol (k_2), although less than thermal relaxation (k_{-1}) is greater than the rate of oxidation of solvent or ethylbenzene (k_3). The photokinetic control (*i.e.* balance of k_1 and k_{-1}) also rationalises the relatively modest observed effect of deuteration in the case of both cyclohexanol and benzyl alcohol (Fig. S11 and S12, ESI[†]), which leads to an underestimation KIE for the reaction of **1**^{*} with the alcohol (Scheme 2). Analysis of the product mixture obtained from irradiation of a 1:1 mixture of benzyl alcohol and 1,1-D₂-benzylalcohol indicates that the KIE is *ca.* 1.5 (Fig. S13, ESI[†]), in agreement with the KIE obtained by a comparison of rates.

In methanol, the effect of near UV irradiation on **1** (Fig. 6 and Fig. S14, ESI[†]) is readily apparent with an estimated quantum efficiency of *ca.* 0.14 (see ESI[†]) and as with acetonitrile, at -30°C solvent deuteration has no effect on the rate of reduction of **1** (CH_3OH vs. CD_3OD , Fig. S15, ESI[†]). The primary photo product at room temperature is the low spin Fe^{III} complex $[(\text{N4Py})\text{Fe}^{\text{III}}-\text{OCH}_3]^{2+}$ (X-band EPR at 77 K, $g = 2.29, 2.12, 1.96$).¹² That the final oxidation state is Fe^{III} and not Fe^{II} , as is the case in acetonitrile, is expected given the large (*ca.* 0.6 V) difference in the $\text{Fe}^{\text{III}}/\text{Fe}^{\text{II}}$ redox potentials of the methanol and acetonitrile bound complexes.

At -30°C , disproportionation is suppressed and the Fe^{II} complex forms concomitant with the decrease in the absorbance due to **1**. Oxidation of methanol to methanol under photo-irradiation proceeds with *ca.* 64% efficiency (determined colourimetrically, 0.32 equiv. CH_2O w.r.t. to **1**, see ESI[†] for details).

The various reactions of importance in the photo-activation of **1** towards substrate oxidation are shown in Scheme 2.

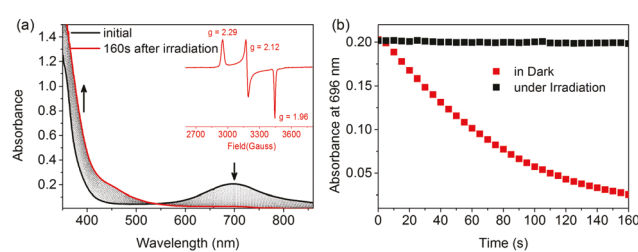


Fig. 6 (a) UV-vis absorption spectrum of **1** (0.5 mM) in CD_3OD at 20°C before (black) and during (dashed lines) irradiation at 365 nm; final spectrum (red). Inset: X-Band EPR spectrum of flash frozen solution at 77 K. (b) Absorbance at 692 nm of **1** over time without (black, initial slope $4.9 \times 10^{-5} \text{ s}^{-1}$) and with irradiation (red, initial slope $1.9 \times 10^{-3} \text{ s}^{-1}$).

The overall rate of decay in the absorbance of **1** (or **2**, **3**) in acetonitrile is determined by photon flux, *i.e.* k_1 , and the concentration of **1*** is limited by a combination of non-radiative relaxation of the excited state (k_{-1}) as well as the rate constants for reaction with and concentration of oxidizable substrates (k_3 and k_5). Although reaction with alcohols proceeds more rapidly than with acetonitrile (*i.e.* $k_2 \gg k_3$), the overall rate of reaction is dominated by k_1/k_{-1} . In the presence of, for example, benzyl alcohol, the reaction goes primarily *via* oxidation of the alcohol (manifested in the concomitant formation of **1a**); the extent of the background reaction with acetonitrile is reduced by the decrease in the excited state lifetime of **1***.

Most reported $\text{Fe}^{\text{IV}}=\text{O}$ complexes have $S = 1$ ground states with a strong $\text{Fe}=\text{O}$ double bond character (bond distance *ca.* 1.65 Å).¹³ Their reactivity towards substrates depends strongly on their ligand environments, with $[(\text{N}4\text{Py})\text{Fe}^{\text{IV}}=\text{O}]^{2+}$ (**1** in Fig. 1) and $[(\text{Bn-TPEN})\text{Fe}^{\text{IV}}=\text{O}]^{2+}$ (**3**) showing surprising stability but nevertheless engaging in C–H bond oxidation, including oxidising cyclohexane at room temperature.⁷ The excited state reached upon visible-NIR excitation is shown, in the present study, not to lead to reduction of **1** nor C–H bond oxidation. In contrast, excitation into the more intense near-UV LMCT bands results in photoinduced reduction. The absorption spectrum of **1** has been characterised earlier by Solomon and co-workers in detail by magnetic circular dichroism (MCD) spectroscopy coupled with DFT calculations.¹⁴ The NIR bands of **1** between 580 to 900 nm are assigned to mixing of formally forbidden $d_{(x^2-y^2)} \leftarrow d_{(xz/yz)}$ transitions with ligand(oxido)-to-metal charge-transfer (LMCT) (from the equatorial nitrogens to the $d_{(x^2-y^2)}$ orbital) transitions. The near-UV band was assigned as a LMCT band with charge transferred from the pyridine π MOs to the $\text{Fe}-\text{O}$ π^* orbitals ($d_{(xz/yz)} \leftarrow \pi_{\text{pyr}}$ charge transfer), resulting in a weakening and hence elongation of the $\text{Fe}(\text{IV})=\text{O}$ bond and an increase in its oxyl radical character, making it a more powerful C–H bond abstracting agent.

In conclusion, we have shown that near UV excitation of a series of non-heme $\text{Fe}^{\text{IV}}=\text{O}$ complexes results in a dramatic enhancement of their reactivity towards C–H activation. The decay kinetics and wavelength dependence indicate strongly that it is a relatively long lived (0.1 to 5 ns)¹⁵ LMCT state that is involved and not the d–d excited states accessed by visible excitation. In light of the emergence of the field of photo-redox catalysis and especially the use of Ru(II) polypyridyl complexes as photo-oxidants to generate $\text{Fe}^{\text{IV}}=\text{O}$ species in solution,¹⁶ the present study raises the possibility that the initially formed $\text{Fe}^{\text{IV}}=\text{O}$ species (*e.g.*, **1**) is in fact formed as **1*** and hence the intrinsic reactivity may be different from that expected for *ex situ* prepared **1**. Furthermore, the use of near-UV light opens the possibility to directly enhance the reactivity of such complexes.

Caution. When working with perchlorate salts, suitable protective safeguards should be in place at all times due to the

risk of explosion. Perchlorate salts should be handled in small (mg) quantities and used only where necessary.

The Ministry of Education, Culture and Science of the Netherlands (Gravity program 024.001.035, WRB), Ubbo Emmius fund (AD) and the Chinese Scholarship Council (JC) are acknowledged for financial support, as is the US National Science Foundation for work carried out in Minnesota (CHE1665391, LQ).

Conflicts of interest

There are no conflicts to declare.

Notes and references

‡ $\text{N}4\text{Py} = (1,1\text{-di}(\text{pyridin}-2\text{-yl})-\text{N},\text{N}\text{-bis}(\text{pyridin}-2\text{-ylmethyl})\text{methanamine}$), $\text{MeN}4\text{Py} = 1,1\text{-di}(\text{pyridin}-2\text{-yl})-\text{N},\text{N}\text{-bis}(\text{pyridin}-2\text{-ylmethyl})\text{ethan-1-amine}$, and $\text{Bn-TPEN} = \text{N-benzyl-}N,\text{N}',\text{N}'\text{-tris}(2\text{-pyridylmethyl})\text{-1,2-diaminoethane}$. § Complexes **2** and **3** show moderately higher rates of thermal reduction in CH_3CN than does **1**, but nevertheless photo-reduction to the corresponding Fe^{II} complexes upon irradiation at 365 nm proceeds substantially more rapidly than the thermal reactions in all cases.

¶ **1** oxidises methanol *via* α -C–H bond cleavage (HAT), manifested in a decrease in absorbance at 696 nm, increase in absorbance below 530 nm and the formation of formaldehyde. The thermal reaction between **1** and methanol at room temperature is essentially stopped by deuteration (CD_3OD) due to the large KIE (~ 50) for HAT.¹⁷

- 1 J. Šima and J. Makáňová, *Coord. Chem. Rev.*, 1997, **160**, 161–189.
- 2 A. J. Allmand and W. W. Webb, *J. Chem. Soc.*, 1929, 1518–1531.
- 3 A. W. Adamson, W. L. Waltz, E. Zinato, D. W. Watts, P. D. Fleischauer and R. D. Lindholm, *Chem. Rev.*, 1968, **68**, 541–585.
- 4 J. England, Y. Guo, E. R. Farquhar, V. G. Young, E. Münck and L. Que, *J. Am. Chem. Soc.*, 2010, **132**, 8635–8644.
- 5 A. Company, G. Sabena, M. González-Béjar, L. Gómez, M. Clémancey, G. Blondin, A. J. Jasniewski, M. Puri, W. R. Browne, J.-M. Latour, L. Que, M. Costas, J. Pérez-Prieto and J. Lloret-Fillol, *J. Am. Chem. Soc.*, 2014, **136**, 4624–4633.
- 6 H. Kotani, T. Suenobu, Y.-M. Lee, W. Nam and S. Fukuzumi, *J. Am. Chem. Soc.*, 2011, **133**, 3249–3251.
- 7 J. Kaizer, E. J. Klinker, N. Y. Oh, J. U. Rohde, W. J. Song, A. Stubna, J. Kim, E. Münck, W. Nam and L. Que, *J. Am. Chem. Soc.*, 2004, **126**, 472–473.
- 8 H. Hirao, D. Kumar, L. Que and S. Shaik, *J. Am. Chem. Soc.*, 2006, **128**, 8590–8606.
- 9 A. Draksharapu, Q. Li, G. Roelfes and W. R. Browne, *Dalton Trans.*, 2012, **41**, 13180–13190.
- 10 A. Draksharapu, Q. Li, H. Logtenberg, T. A. van den Berg, A. Meetsma, J. S. Killeen, B. L. Feringa, R. Hage, G. Roelfes and W. R. Browne, *Inorg. Chem.*, 2011, **51**, 900–913.
- 11 N. Y. Oh, Y. Suh, M. J. Park, M. S. Seo, J. Kim and W. Nam, *Angew. Chem., Int. Ed.*, 2005, **44**, 4235–4239.
- 12 G. Roelfes, M. Lubben, K. Chen, R. Y. N. Ho, A. Meetsma, S. Genseberger, R. M. Hermant, R. Hage, S. K. Mandai, V. G. Young Jr., Y. Zang, H. Kooijman, A. L. Spek, L. Que Jr. and B. L. Feringa, *Inorg. Chem.*, 1999, **38**, 1929–1936.
- 13 A. R. McDonald and L. Que, *Coord. Chem. Rev.*, 2013, **257**, 414–428.
- 14 A. Decker, J.-U. Rohde, E. J. Klinker, S. D. Wong, L. Que and E. I. Solomon, *J. Am. Chem. Soc.*, 2007, **129**, 15983–15996.
- 15 S. Schenker, P. C. Stein, J. A. Wolny, C. Brady, J. J. McGarvey, H. Toftlund and A. Hauser, *Inorg. Chem.*, 2001, **40**, 134–139.
- 16 H. Kotani, T. Suenobu, Y.-M. Lee, W. Nam and S. Fukuzumi, *J. Am. Chem. Soc.*, 2011, **133**, 3249–3251.
- 17 N. Y. Oh, Y. Suh, M. J. Park, M. S. Seo, J. Kim and W. Nam, *Angew. Chem.*, 2005, **117**, 4307–4311.